Molecules interacting with a metallic nanowire

M. Boustimi,[1] J. Baudon,[2,*] and J. Robert[2]
[1]*Laboratoire d'Optronique (UMR-CNRS), ENSSAT, 6 rue de Kérampon, BP 447, 22305-Lannion Cedex, France*
[2]*Laboratoire de Physique des Lasers (UMR-CNRS 7538), Université Paris 13, Av. J.B. Clément, 93430-Villetaneuse, France*

(Received 18 June 2002; revised manuscript received 12 November 2002; published 27 January 2003)

General expressions for inductive and dispersive dipolar contributions to the van der Waals interaction between a molecule and a metallic or dielectric nanowire are given. The nonlocal response of the metal is modeled by a standard hydrodynamic dielectric function, which provides exact and analytical expressions for the reflection factors. Numerical calculations are carried out for a HF molecule located at a mean distance from an aluminum wire. A nonpolar molecule (N_2) is then considered in order to avoid any chemisorption effect. The anisotropy of the dispersive van der Waals potential is responsible for rotational transitions of molecules passing in the vicinity of the wire, giving rise to a rotational alignment.

DOI: 10.1103/PhysRevB.67.045407 PACS number(s): 68.49.Df, 34.50.Dy, 34.50.Ez

I. INTRODUCTION

The interaction between an *atom* and a mesoscopic solid at short and intermediate distances, i.e., from 0.1 up to a few hundreds of nm, exhibits special features originating from the small size of the solid itself or of the structures it holds, such as curvature effects, nonlocality of the solid response, etc.[1] These effects are mainly observed at intermediate distances (1–100 nm) where the interaction is of the van der Waals (vdW) type. Retardation effects appearing at larger distances[2] can generally be ignored because of their smallness and the difficulty to observe them experimentally. Actually, the interaction also strongly depends on the internal state of the atom. For a physisorbed ground-state atom, the vdW potential combines with a short-range potential due to the overlap of electronic orbitals, giving rise to a potential well and either a trapping of the atom or a rainbow effect.[3] For metastable atoms, the polarizability as well as the vdW constant is larger than for the ground state, which strongly affects the elastic scattering by surfaces and modifies the intensities scattered by a nanoslit grating.[4] It has been also shown that for excited atoms the vdW interaction is strongly affected by the solid excitation modes[5] and that this interaction can take a nondiagonal character, breaking the atomic-state symmetry and inducing fine-structure transitions.[6] The case of *molecules* is obviously more complex, even for diatomic molecules to which the present paper will be restricted, because of additional degrees of freedom associated with vibrational and rotational motions. In spite of the interest of considering electronically excited metastable molecules, such as $N_2^*(^3\Sigma_u^+)$, in which the vdW interaction induces vibrational transitions,[7] we shall assume here a well-defined vibrational state and only consider rotational states affected by the anisotropy of the interaction, which is justified for ground-state (and less polarizable) molecules. Another important difference of molecules compared to atoms is the possibility for heteronuclear molecules to carry a permanent electric dipole, which gives an additional anisotropic inductive contribution to the interaction energy. From a general point of view, detailed knowledge of the interaction of molecules of any kind, excited or not, with small-sized solids or structures, such as spheres, bubbles, wires, tubes, stripes on various substrates, etc., is of great importance in the understanding of the physisorption (or chemisorption) on this kind of surfaces and more generally of the molecular physics within such confined geometry[8]—for instance, for a single molecule under the tip of an optical, photoion, or scanning tunneling microscopy (STM) near-field microscope.[9] Up to now, a great deal of theoretical and experimental effort has been devoted to the study of atoms and molecules in various confined environments, generally in view to store or trap them, perform a state selection in collision experiments, or use them in an interferometer. So far, systems of wires and microchips have been developed for atoms and even atomic Bose-Einstein condensates[10] and wires, quadrupolar traps, and storage rings for polar molecules.[11] While most of these devices consist of charged electrodes or currents, it is likely that the van der Waals interaction plays a more and more important role as the size of such systems, or the distance of closest approach, is made smaller and smaller.

The scope of the present paper is necessarily limited compared to the ambitious program mentioned before. Nevertheless, it will be seen that the study of simple diatomic ground-state molecules interacting with metallic (or dielectric) wires of small radius (a few nm) gives insight into essential features of this interaction. In particular, the evolution of the rotational states in the vicinity of the nanowire is of interest insofar as it can lead to a rotational alignment of the trapped or scattered molecules. The organization of the paper will be as follows: in Sec. II, the theory of the vdW interaction of molecules, possessing or not a permanent dipole moment, with a metallic cylindrical solid is presented. This general treatment, which uses the so-called *eigenmode* method, leads to exact and analytical results within the framework of our hypotheses: namely, no retardation effect, linearity of the response, and hydrodynamic model for the dielectric function of the solid.[12] It is then applied to the calculation of vdW potential surfaces for some molecule-metal systems. In Sec. III, these results are used to study the dynamics of molecules in the vicinity of the wire, especially the evolution of rotational states. Conclusions and perspectives are finally presented in Sec. IV.

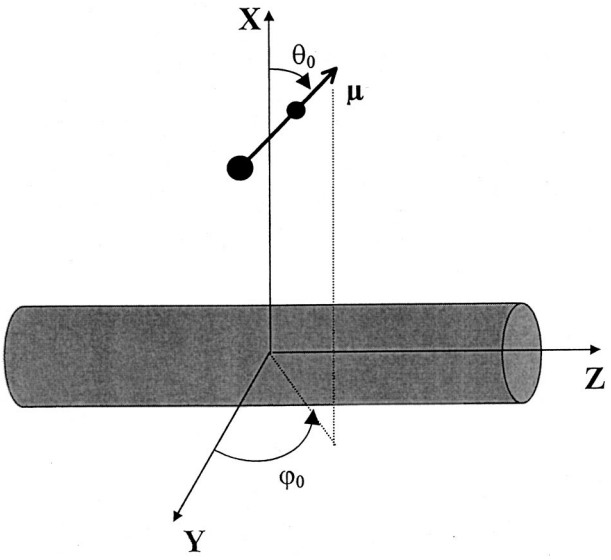

FIG. 1. Geometry of the problem. The cylindrical wire the axis of which is Z has a radius a. The center of mass of the molecule is on the X axis at a distance R from the origin. The internuclear axis $\hat{r}$ has polar angles θ_0, φ_0 referred to the X axis. The origin $\varphi_0=0$ is taken along the Y axis.

II. MOLECULE-NANOWIRE van der WAALS INTERACTION

A. Response of the solid

The metallic or dielectric solid is an infinitely long cylinder of radius a, the axis of which is Z. The center of mass of the molecule is located on the X axis, at a distance $R>a$ from the Z axis. The internuclear axis $\mathbf{r}$ of the molecule is oriented along the z axis whose polar and azimuthal angles referred to X are, respectively, θ_0 and φ_0 (see Fig. 1), the laboratory frame for the molecule being (Y, Z, X). The origin $\varphi_0=0$ has been chosen along Y. While higher-order multipoles could be easily introduced, for the sake of clarity we shall restrict our discussion to *dipole* moments: namely, the permanent dipole $\boldsymbol{\mu}$ (if any) collinear to $\mathbf{r}$ and a fluctuating dipole, which are respectively responsible for the inductive (U_i) and the dispersive (U_d) parts of the interaction.

The method previously used in the case of an atom interacting with a nanowire[13] can be used here as well to evaluate the response potential and field of the solid, the main differences, exclusively due to the source term, being the existence of a permanent dipole (involving a special contribution of the zero frequency), and a more complicated expression of the polarizability. The basic idea in this method is to expand, at a given frequency, the potential Φ_1 inside the solid over a complete basis set of orthogonal functions adapted to the geometry (the *eigenmodes* of the problem): namely, $J_n(k_\perp\rho)\exp(in\varphi)\exp(ik_\parallel z)$, where ρ, φ, Z are cylindrical coordinates. These modes obey the Helmholtz equation and are submitted to the boundary condition $[dJ_n(k_\perp\rho)/d\rho)]_{\rho=a}=0$, which leads to a discrete spectrum of the transverse momentum $k_\perp$. Similarly, the source and response potentials $\Phi_{s,r}$ are expanded over the basis set $I(\text{or } K)_n(k_\parallel\rho)\exp(in\varphi)\exp(ik_\parallel z)$, where $I(\text{or } K)_n$ are modified Bessel functions. Owing to the linearity of the relationship between the charge density induced in the solid and Φ_1, a bipoint susceptibility function can be introduced, which is expressed in the eigenmode basis as a matrix (diagonal in n and $k_\parallel$ because of the cylindrical symmetry): $\chi(k_\parallel,k_\perp,k'_\perp,\omega)$. Then boundary conditions at $\rho=a$ lead to the determination of the so-called *reflection factors*

$$\Delta_n(k_\parallel,a,\omega)=\frac{K'_n(k_\parallel a)}{I'_n(k_\parallel a)}\frac{R_n(k_\parallel)}{A_n(k_\parallel)},$$

where R_n and A_n are the coefficients in the expansions of Φ_r and Φ_s, respectively, $K'(I')$ being the derivatives of functions $K(I)$. The calculation, already developed in Ref. 13, leads to

$$\Delta_n(k_\parallel,a,\omega)=-\frac{I_n(k_\parallel a)-k_\parallel F_n(k_\parallel,a,\omega)I'_n(k_\parallel a)}{K_n(k_\parallel a)-k_\parallel F_n(k_\parallel,a,\omega)K'_n(k_\parallel a)}\frac{K'_n(k_\parallel a)}{I'_n(k_\parallel a)}, \tag{1}$$

where

$$F_n(k_\parallel,a,\omega)=a\sum_{k_\perp,k'_\perp=0}^{+\infty}B_n(k_\perp)B_n(k'_\perp)J_n(k_\perp\rho)\times J_n(k'_\perp a)E_n^{-1}(k_\parallel,k'_\perp,k_\perp,\omega), \tag{2}$$

$B_n(k_\perp)$ are normalization factors the detailed expression of which is not necessary here, and

$$E_n=-4\pi\chi(k_\parallel,k_\perp,k'_\perp,\omega)+(k_\parallel^2+k_\perp^2)\delta_{k'_\perp,k_\perp}. \tag{3}$$

In the usual case of a nonlocal dielectric function of the hydrodynamic type,

$$\varepsilon(k,\omega)=1-\frac{\omega_p^2}{\omega^2-\delta^2(k_\parallel^2+k_\perp^2)}, \tag{4}$$

where ω_p is the plasma frequency and δ the nonlocal parameter, an *exact* and *analytical* expression of the F_n functions can be obtained, by a method similar to that already used for a metallic nanosphere:[14]

$$F_n(k_\parallel,\rho,i\xi)=\frac{\xi^2}{\xi^2+\omega_p^2}\frac{I_n(k_\parallel\rho)}{k_\parallel I'_n(k_\parallel a)}+\frac{\omega_p^2}{\xi^2+\omega_p^2}\frac{I_n(\beta\rho)}{\beta I'_n(\beta a)}, \tag{5}$$

where $\beta=[(\xi^2+\omega_p^2)/\delta^2+k_\parallel^2]^{1/2}$ and $i\xi$ is a complex frequency.

Just as in the case of an atom in the vicinity of a wire,[13] the case of a dielectric cylinder is readily found by making $\delta=0$ (local response of the solid) and using a dielectric constant $\varepsilon(\omega)$ of a form rather similar to Eq. (4) (e.g., Clausius-Mossotti formula). In that case one obtains again an analytical form of the reflection factors, a form which is actually identical to that already given in the previous reference:

$$\Delta_n^{\text{loc}}=\frac{[\varepsilon(\omega)-1]I_n(k_\parallel a)K'_n(k_\parallel a)}{I_n(k_\parallel a)K'_n(k_\parallel a)-\varepsilon(\omega)I'_n(k_\parallel a)K_n(k_\parallel a)}, \tag{5'}$$

where I_n, K_n are Bessel functions and I_n', K_n' their derivatives.

B. vdW potential energy surface

In a general case, once the response potential $\Phi_r(\mathbf{r},\omega)$ induced by a source located at point $\mathbf{r}'$, the mth-order momentum of which is $\mathbf{M}^{(m)}$ is known, its successive gradients $\mathbf{E}_n(\mathbf{r},\omega)$ are readily obtained using the so-called *propagators*:[15]

$$\mathbf{E}_n(\mathbf{r},\omega)=-[(2m-1)!!]^{-1}\,{}^n\mathbf{S}^m(\mathbf{r},\mathbf{r}',\omega)(\cdot)^m\mathbf{M}^{(m)}(\omega), \tag{6}$$

where ${}^n\mathbf{S}^m$ is a tensor of rank $(n+m)$ and $(\cdot)^m$ is a contracted product. As mentioned before, we shall restrict our discussion to the dominant dipolar contributions, i.e., terms such as $n=m=1$. Hence the source momentum is the permanent dipole $\boldsymbol{\mu}$ (if any) and a fluctuating molecular dipole. The permanent dipole gives rise to the inductive potential energy[16]

$$U_i=-\frac{1}{2}[(\mu_X)^2\,{}^1S^1_{XX}+(\mu_Y)^2\,{}^1X^1_{YY}+(\mu_Z)^2\,{}^1S^1_{ZZ} +2\mu_Y\mu_Z\,{}^1S^1_{YZ}]. \tag{7}$$

All terms of ${}^1\mathbf{S}^1$ are taken at $\mathbf{r}=\mathbf{r}'=\mathbf{R}$ and $\omega=0$. We have

$$\begin{aligned}
{}^1S^1_{YY}&=\frac{1}{\pi}\sum_{n=-\infty}^{+\infty}\int_{-\infty}^{\infty}dk_\parallel\frac{n^2}{R^2}K_n^2(k_\parallel R)G_n(k_\parallel,a,0),\\
{}^1S^1_{XX}&=\frac{1}{\pi}\sum_{n=-\infty}^{+\infty}\int_{-\infty}^{\infty}dk_\parallel k_\parallel^2K_n'^2(k_\parallel R)G_n(k_\parallel,a,0),\\
{}^1S^1_{ZZ}&=\frac{1}{\pi}\sum_{n=-\infty}^{+\infty}\int_{-\infty}^{\infty}dk_\parallel k_\parallel^2K_n^2(k_\parallel R)G_n(k_\parallel,a,0),\\
{}^1S^1_{YZ}&=\frac{1}{\pi}\sum_{n=-\infty}^{+\infty}\int_{-\infty}^{\infty}dk_\parallel\frac{nk_\parallel}{R}K_n^2(k_\parallel R)G_n(k_\parallel,a,0),
\end{aligned} \tag{8}$$

with

$$G_n=\Delta_n\frac{I_n'(k_\parallel a)}{K_n'(k_\parallel a)}. \tag{9}$$

Finally,

$$U_i=-\frac{\mu^2}{\pi}(I_1+I_2\cos^2\theta_0+I_3\sin^2\theta_0\cos 2\varphi_0). \tag{10}$$

The coefficients $I_{1,2,3}$ (which are only R dependent) are given by

$$\begin{aligned}
I_1&=\sum_{n=-\infty}^{+\infty}\int_0^{\infty}dk_\parallel\frac{1}{2}\left(\frac{n^2}{R^2}+k_\parallel^2\right)K_n^2(k_\parallel R)G_n(k_\parallel,a,0),\\
I_2&=\sum_{n=-\infty}^{+\infty}\int_0^{\infty}dk_\parallel\left[k_\parallel^2K_n'^2(k_\parallel R)-\frac{1}{2}\left(\frac{n^2}{R^2}+k_\parallel^2\right)K_n^2(k_\parallel R)\right]G_n(k_\parallel,a,0),\\
I_3&=\sum_{n=-\infty}^{+\infty}\int_0^{\infty}dk_\parallel\frac{1}{2}\left(\frac{n^2}{R^2}-k_\parallel^2\right)K_n^2(k_\parallel R)G_n(k_\parallel,a,0).
\end{aligned} \tag{11}$$

Finally, the dispersive part of the interaction is[16,17]

$$U_d=\frac{\hbar}{2\pi}\int_0^{+\infty}d\xi\,{}^1\alpha^1(i\xi)(\cdot)^2\,{}^1\mathbf{S}^1(\mathbf{R},\mathbf{R},i\xi), \tag{12}$$

where ${}^1\alpha^1$ is the polarizability tensor of the molecule. In the molecular frame (x, y, z), where $\hat{z}$ is along $\mathbf{r}$, it is represented by a diagonal matrix of elements $\alpha_\parallel$, $\alpha_\perp$, $\alpha_\perp$, where $\alpha_{\parallel,\perp}$ are the parallel and perpendicular polarisabilities. It is transformed into the fixed frame (X, Y, Z) by a rotation involving the Euler angles φ_0, θ_0, 0. Then Eq. (12) becomes

$$U_d=\frac{\hbar}{2\pi}\int_0^{\infty}d\xi(\alpha_{XX}\,{}^1S^1_{XX}+\alpha_{YY}\,{}^1S^1_{YY}+\alpha_{ZZ}\,{}^1S^1_{ZZ} +2\alpha_{YZ}\,{}^1S^1_{YZ}). \tag{13}$$

The elements of ${}^1\mathbf{S}^1$ are given by Eq. (8) where the frequency is now $i\xi$ instead of zero. Then one obtains for U_d an angular dependence identical to that of U_i:

$$U_d=\frac{\hbar}{\pi^2}(D_1+D_2\cos^2\theta_0+D_3\sin^2\theta_0\cos 2\varphi_0), \tag{14}$$

where

$$\begin{aligned}
D_1&=\sum_{n=-\infty}^{\infty}\int_0^{\infty}d\xi\int_0^{\infty}dk_\parallel\left[\frac{1}{2}(\alpha_\parallel+\alpha_\perp)\left(\frac{n^2}{R^2}+k_\parallel^2\right)K_n^2(k_\parallel R) +\alpha_\perp k_\parallel^2K_n'^2(k_\parallel R)\right]G_n(k_\parallel,a,u\xi),\\
D_2&=\sum_{n=-\infty}^{\infty}\int_0^{\infty}d\xi\int_0^{\infty}dk_\parallel(\alpha_\parallel-\alpha_\perp)\left[k_\parallel^2K_n'^2(k_\parallel R) -\frac{1}{2}\left(\frac{n^2}{R^2}+k_\parallel^2\right)K_n^2(k_\parallel R)\right]G_n(k_\parallel,a,i\xi),\\
D_3&=\sum_{n=-\infty}^{\infty}\int_0^{\infty}d\xi\int_0^{-y}dk_\parallel(\alpha_\parallel-\alpha_\perp) \times\left(\frac{n^2}{R^2}+k_\parallel^2\right)K_n^2(k_\parallel R)G_n(k_\parallel,a,i\xi).
\end{aligned} \tag{15}$$

Notice that, for $\alpha_\parallel=\alpha_\perp$, the dispersive interaction becomes isotropic, as expected.

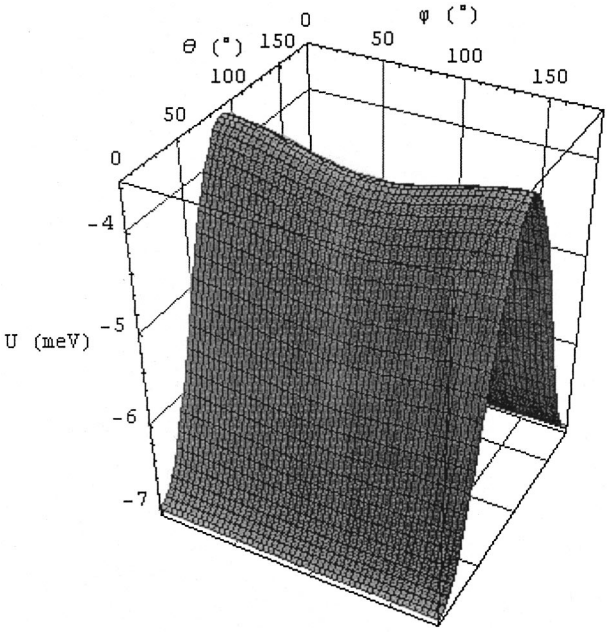

FIG. 2. HF molecule in the vicinity of an aluminum wire (radius $a=40$ a.u.). Total (inductive+dispersive) vdW energy U (in meV) as a function of angles θ_0, φ_0, for $R=52$ a.u.

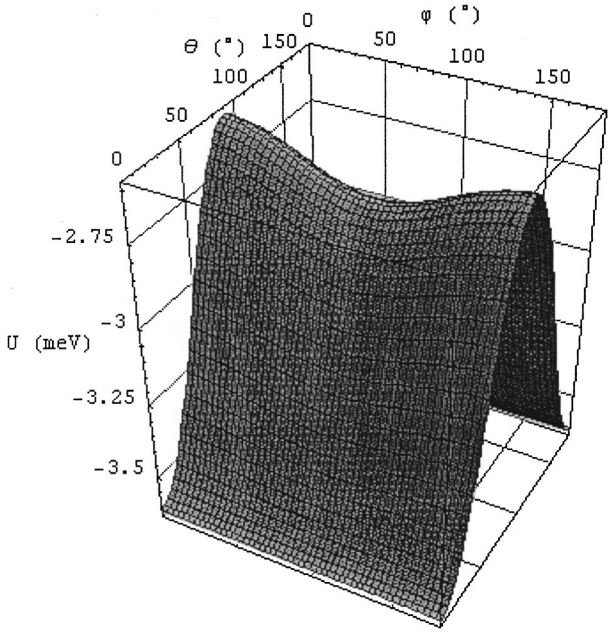

FIG. 3. Same as Fig. 2 for a N_2 molecule in the vicinity of an aluminum nanowire ($a=40$ a.u., $R=52$ a.u.); here, U is a purely dispersive energy.

C. Polar and nonpolar molecules in the vicinity of a metallic nanowire

Inductive and dispersive interactions between a HF molecule and an aluminum wire, of radius $a=40$ a.u., have been calculated using expressions (10), (11) and (14), (15). For the metal the set of parameters (in a.u.) (Ref. 16) $\omega_p=0.562\,66$, $\delta=0.697$ is used. For the HF molecule,[16] $\mu=1.78$ and $\alpha_{\parallel,\perp}(\omega)=\alpha_{\parallel,\perp}(0)\omega_{\parallel,\perp}^2/(\omega_{\parallel,\perp}^2-\omega^2)$ (Drude model), with $\alpha_{\parallel}(0)=5.2$, $\alpha_{\perp}(0)=3.84$, $\omega_{\parallel}=1.561$, and $\omega_{\perp}=0.375$. Figure 2 shows the dependence of the total vdW interaction U on angles θ_0 and φ_0 for $R=52$ a.u., i.e., at a distance $d=12$ a.u. ($=0.635$ nm) from the solid. A strong anisotropy with respect to θ_0 is observed ($\Delta U/\overline{U}\approx 63.5\%$) and a much smaller one with φ_0 ($\Delta U/\overline{U}\approx 6.75\%$). For $\theta_0=\pi/2$ the dependence of both U_i and U_d on φ_0 was expected: the polarizability of the wire is higher in the direction of its axis Z than it is in any direction perpendicular to Z. Hence the magnitude $|U|$ of the interaction is smaller at $\varphi_0=0$ (molecular axis perpendicular to Z) than it is at $\varphi_0=\pi/2$ (molecular axis parallel to Z). This effect is more marked for the inductive part at larger distances. For instance, at $R=140$ a.u. one obtains $U_\iota=-1.0529\times10^{-3}$ meV in the former situation and -3.284×10^{-3} meV in the latter one, whereas U_d increases by only 10%. In the mean distance range (10–300 a.u.) the dependence of the isotropic part of the interaction $U_1=I_1+D_1$ on the distance d follows the law $d^{-3}\,(1+0.022d)$ (d in a.u.). At short distance it is similar to that calculated previously for an atom near a large-radius wire.[13] Moreover, the present calculation shows approximately the same dependence on d of the anisotropy coefficients $U_{2,3}=I_{2,3}+D_{2,3}$.

Only the dispersive interaction is present in the case of a symmetric nonpolar molecule such as N_2. The calculation of U_d for the N_2/Al system has been carried out using for the metal the parameters given previously and for the molecule (in a.u., at the equilibrium distance): $\alpha_{\parallel}(0)=10.286$, $\alpha_{\perp}(0)=3.416$, and $\omega_{\parallel}=\omega_{\perp}=1.10$. It is seen in Fig. 3 that the θ_0 anisotropy at $R=52$ a.u. (about 30%) is lower than the previous one, whereas the φ_0 anisotropy is comparable to ($\Delta U/\overline{U}\approx 5.5\%$). At the mean distance, the common dependence on d of the coefficients, in $d^{-3}\,(1+0.014d)$ (d in a.u.) also holds for the N_2 molecule. This greatly simplifies the treatment of the dynamics.

III. MOLECULAR DYNAMICS

A. Evolution of rotational states

Let us consider a N_2 molecule the center of mass (c.m.) of which follows, at a constant velocity v, a classical rectilinear trajectory perpendicular to the Z axis. This statement implies that (i) a classical description of the c.m. motion is valid, i.e., that the de Broglie wavelength is small compared to the range of the interaction; this is widely verified at thermal energies (a few tens of meV); (ii) the deflection due to the vdW potential is small, which is verified at sufficiently large impact parameters. Actually, this second hypothesis is not strictly necessary for the following semiclassical treatment. Indeed, at sufficiently large impact parameters ($\rho>12$ a.u.) the classical deflection angle Θ is small enough ($\Theta<15°$) to allow us to consider the internal molecular evolution as taking place along a straight line trajectory. Then—and without any contradiction—one can use the dependence of Θ on ρ to calculate transition probabilities, differential cross sections, etc., as functions of Θ. A third hypothesis in our treatment is that the electronic (ground state) and vibrational ($v=0$) states of the molecule remain unchanged during the collision,

which appears to be reasonable for not too large incident energies (in the present case $E_0 \leqslant 50$ meV). Under these conditions the only internal degrees of freedom involved here are θ_0 and φ_0. They correspond to the rotation of the molecule which will be assimilated to a rigid rotator (more intricate situations could be treated as well along the same principles). Then the rotational wave functions $|J,M\rangle$, where J is the angular momentum and M its projection on the fixed Z axis, are simply the spherical harmonics $Y_J^M(\theta_0,\varphi_0)$. Owing to the symmetry of the molecule, a single parity of J is allowed, J being even for the electronic ground state. The angular dependence of U_d [Eq. (14)] can be written as well as an expansion over spherical harmonics:

$$U_d = -\{d_1 Y_0^2(\hat{r}) + d_2 Y_2^0(\hat{r}) + d_3[Y_2^{+2}(\hat{r}) + Y_2^{-2}(\hat{r})]\}, \tag{16}$$

where

$$d_1 = \sqrt{4\pi}(D_1 + D_2/3), \quad d_2 = 4\sqrt{\frac{\pi}{5}} D_2,$$

$$d_3 = 2\sqrt{\frac{2\pi}{15}} D_3. \tag{17}$$

Let H_0 be the rotational Hamiltonian of the isolated molecule. In the vicinity of the wire it becomes $H = H_0 + U_d$, and the rotational wave function $|\psi\rangle$ obeys the time-dependent Schrödinger equation

$$i\hbar\,\partial_t|\psi\rangle = (H_0 + U_d)|\psi\rangle. \tag{18}$$

Expanding $|\psi\rangle$ over the free rotational states and replacing in Eq. (18), one gets for the amplitudes a_{JM} a set of coupled equations

$$i\hbar\,\dot{a}_{JM} = \sum_{J'M'} \langle JM|U_d|J'M'\rangle a_{J'M'}, \tag{19}$$

where $\dot{a}$ is the time derivative of a. Using Eqs. (16) and (19), the selection rule $M' - M = 0, \pm 2$ is readily derived. In order to simplify the resolution of Eq. (19) and avoid useless complications we shall assume that the initial rotational state is $|0,0\rangle$. Under such conditions the problem reduces to four states: namely, $|0,0\rangle$, $|2,0\rangle$, $|2,+2\rangle$, $|2,-2\rangle$. In fact, states $|2,\pm 2\rangle$ obey the same differential equation. Then (provided that the initial conditions are adequate), only the state $(1/\sqrt{2})(|2,+2\rangle + |2,-2\rangle)$ has to be considered, which reduces the number of states to 3. These states will be labeled 1, 2, 3. As all coefficients in U_d have the same dependence on d, this also holds for its matrix elements which can be written in the form $f[d(t)]\,W_{jk}$, all terms W_{jk} being constant. Let us introduce the new variable

$$u(t) = \int_{-\infty}^{t} dt' f[d(t')], \tag{20}$$

where $d = [(a+\rho)^2 + v^2 t^2]^{1/2} - a$, with $\rho = d(0)$ the impact parameter. At mean distances $f \approx (12/d)^3\ (1 + 0.014d)^{-1}$ ($d = 12$ a.u. being simply an arbitrary reference distance), then Eq. (19) reduces into

$$i\hbar\,\dot{a}_j' = \sum_{k=1}^{3} W_{jk} a_k, \tag{21}$$

where $a_j' = da_j/du$. As the elements W_{jk} are constant, $|\psi\rangle$ can be reexpanded over the time-independent eigenvectors of $\mathbf{W}$ with new amplitudes $b_n(u)$ given by

$$b_n(u) = b_n(0)\exp(-iw_n u) \quad (n = 1,2,3). \tag{22}$$

The $w_n - s$ are the eigenvalues of $\mathbf{W}$. With our parameters, we find (in a.u.)

$$w_1 = -3.835\,03, \quad w_2 = -2.130\,92, \quad w_3 = -2.034\,39. \tag{23}$$

The initial values $b_n(u=0)$ are derived from those of a_j by a simple rotation $\mathbf{R}$:

$$\mathbf{b}(0) = \mathbf{R}^{-1}\mathbf{a}(0), \tag{24a}$$

$\mathbf{b}$ and $\mathbf{a}$ being the column matrices of amplitudes b_n and a_j. Finally, we obtain

$$a_j(u) = \sum_n A_{jn} \exp(-iw_n u), \tag{24b}$$

where A_{jn} are constant coefficients.

B. Transition probabilities and alignment effect

It is worth noticing that the dependence of the amplitudes on both the velocity and the impact parameter is entirely contained in $u(t)$. From Eq. (20) it is seen that the initial conditions at $t = -\infty$ correspond to $u = 0$, whereas the final amplitudes at $t = +\infty$ correspond to the finite upper limit of u. Figure 4(a) shows an example of the time evolution of populations $|a_j|^2$ at impact parameter $\rho = 15$ a.u. and an incident velocity of 609 m/s (i.e., an incident energies $E_0 = 28.0$ meV), with the initial conditions $a_1 = 1$, $a_2 = 0$, and $a_3 = 0$. Transition probabilities $|a_2|^2$ and $|a_3|^2$ are shown in Fig. 4(b) as functions of ρ. They are clearly different from each other: in the present range of ρ, $|a_2|^2$ is oscillatory, whereas $|a_3|^2$ is a monotonic decreasing function (actually in the whole range of ρ, the behavior of $|a_3|^2$ is similar to that of $|a_2|^2$ apart from scaling factors). This difference means that molecules emerging in states $J = 2$ are rotationally aligned. The degree of alignment, defined as $\alpha = (|a_2|^2 - |a_3|^2)/(|a_2|^2 + |a_3|^2)$, is shown in Fig. 4(c) as a function of the impact parameter. It is an oscillating function tending to $+1$ as $\rho \to \infty$. The minima are sharply peaked because $|a_3|^2$ is much smaller than the amplitude of oscillation of $|a_2|^2$.

Due to the close values of the diagonal terms of $\mathbf{W}$ and to the smallness of the rotational energy (~ 0.4 meV for $J = 2$) compared to E_0, the hypothesis of a common trajectory governed by a mean vdW potential U is justified. For $\rho > 12$ a.u. the (small) classical deflection angle is given by[18]

$$\Theta(\rho) \approx -\frac{2\rho}{E_0}\int_0^{\infty} \partial_R U \frac{dY}{R}, \tag{25}$$

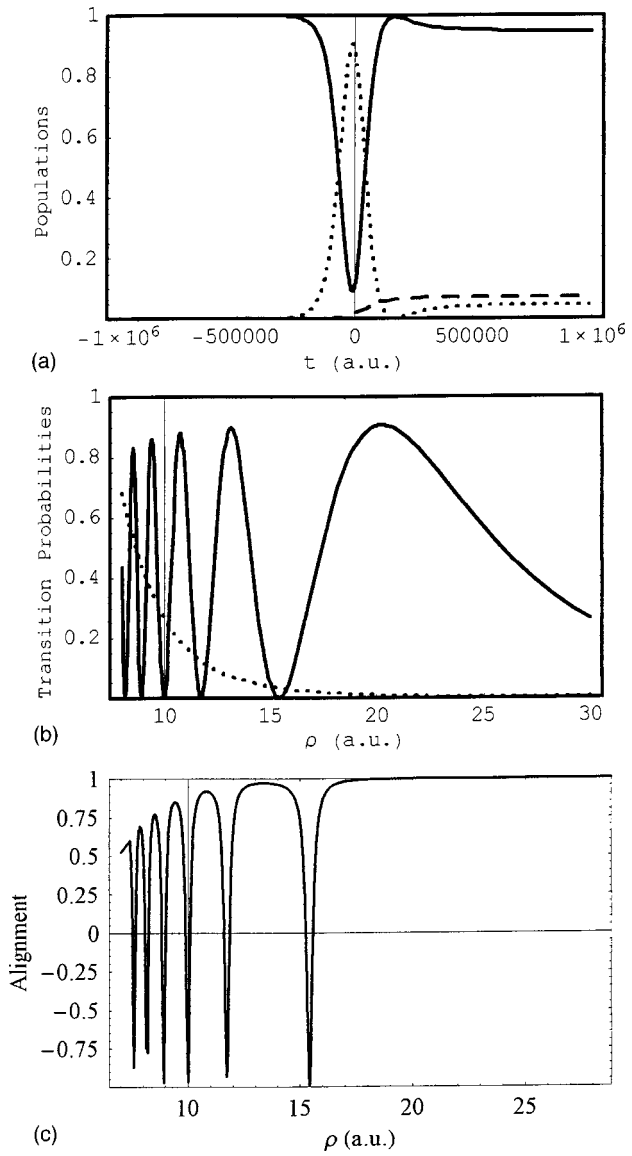

FIG. 4. N_2 molecule colliding with an aluminum nanowire ($a = 40$ nm) at an incident velocity of 609 m/s. (a) Time evolution of rotational populations; time t is in a.u. (1 a.u.$=2.419\times10^{-17}$ s). Solid line: population $|a_1|^2$ in state $|1\rangle=|0,0\rangle$. Short-dashed line: $|a_2|^2$ in state $|2\rangle=|2,0\rangle$. Long-dashed line: $|a_3|^2$ in state $|3\rangle=(1/\sqrt{2})(|2,+2\rangle+|2,-2\rangle)$. (b) Final populations $|a_2|^2$ (solid line) and $10\times|a_3|^2$ (dashed line) as functions of the impact parameter ρ. (c) Degree of alignment $\alpha=(|a_2|^2-|a_3|^2)/(|a_2|^2+|a_3|^2)$ as a function of ρ.

where R is the distance of the molecule center of mass to the Z axis and $\hat{Y}$ is the incident direction. From $\Theta(\rho)$ the differential equation is readily derived: $d\sigma/d\theta=[\partial_\rho\Theta]^{-1}_{\rho_C}$ where ρ_C is the "classical" impact parameter for which $\theta=\Theta(\rho_C)$. Inelastic total cross sections can be calculated as well using $\sigma_{1,2(3)}=\int_0^\infty |a_{2(3)}|^2 d\rho$. At $v=609$ m/s one obtains $\sigma_{12}\approx16$ a.u. and $\sigma_{13}\approx1.4$ a.u. Notice that these cross sections have the dimension of a length since they are implicitly referred to a wire of unit length. Figure 5(a) shows the final populations $|a_2|^2$ and $|a_3|^2$ as functions of the deflection angle. As Θ is a monotonously decreasing function

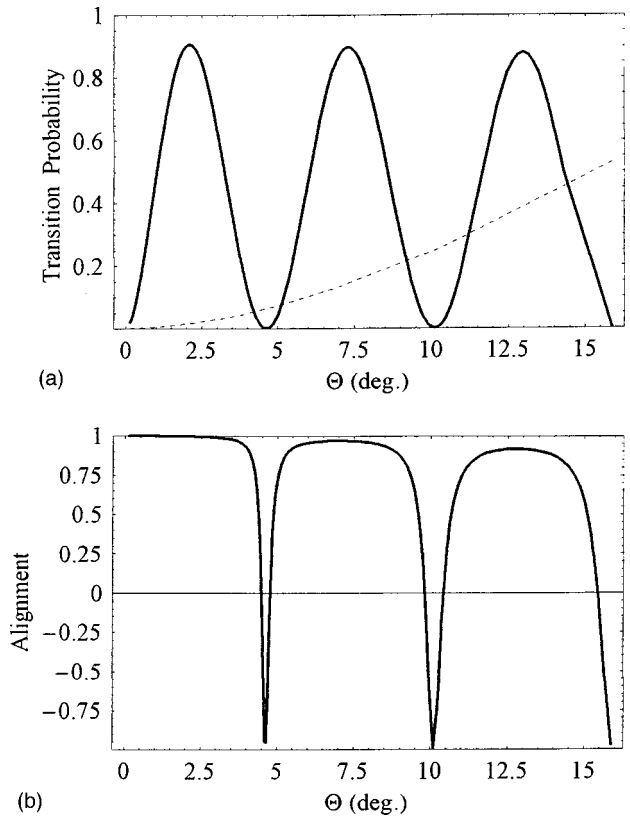

FIG. 5. (a) Same as Fig. 4(b), as functions of the deflection angle Θ (in deg). (b) Same as Fig. 4(c), as a function of the deflection angle Θ (in deg).

of ρ, the former population regularly oscillates with Θ, whereas the latter one is monotonously increasing. This leads to an alignment degree α which oscillates as a function of the angle [Fig. 5(b)], $|\alpha|$ reaching values close to 1 in the present small-angle range. As far as smaller impact parameters are considered, an anisotropic repulsive contribution must be added to the vdW potential. This repulsive potential can be estimated by summing, over the metal lattice, atom (N)–atom (Al) interactions of the form C_{12}/ℓ^{12}, where ℓ is the N-Al distance and $C_{12}\approx1.20\times10^7$ a.u.,[19] the minimum distance between two Al atoms in the lattice being 4.83 a.u. The total potential exhibits an anisotropic potential well. For $\theta_0=0$ it is located at 10.3 a.u. from the surface with a depth $\varepsilon_m=2.5$ meV, and for $\theta_0=\pi/2$, $\varphi_0=\pi/2$, at 8.0 a.u. with a depth of 5 meV. In the present range of impact parameters ($\rho>12$ a.u.) the repulsive part is negligible. Nevertheless, this well *a priori* produces rainbow effects at an angle[20] $|\Theta|\approx2\ \varepsilon_m/E_0\approx20°$ (on average) larger than those considered in our discussion.

If one neglects transitions $J=2\rightarrow4$ (otherwise, the size of the matrix considered below gets larger), then the previous treatment can be carried out for any initial conditions, leading to the linear relationship

$$\mathbf{a}(t=+\infty)=\mathbf{S}\mathbf{a}(t=-\infty), \tag{26}$$

where $\mathbf{S}$ is the scattering matrix. It is given by

$$\mathbf{S}=\mathbf{R}^{-1}\mathbf{E}\mathbf{R}. \tag{27}$$

TABLE I. Coefficients σ_{jkn} appearing in the scattering matrix **S** (see text), in atomic units.

j, k	$n=1$	$n=2$	$n=3$
1,1	0.347870	0.062153	0.589970
1,2	0.476294	-0.045698	-0.430595
1,3	-6.099×10^{-4}	-0.237069	0.237679
2,2	0.652129	0.033601	0.314271
2,3	8.351×10^{-4}	0.174305	-0.173471
3,3	1.07×10^{-6}	0.904247	0.095752

E is a diagonal matrix the elements of which are $E_{nn}=\exp(-i\,w_n u_M)$. Hence,

$$S_{jk}=\sum_n \sigma_{jkn}E_{nn}, \tag{28}$$

where σ_{jkn} are constant coefficients (i.e., independent of v and ρ) given in Table I.

Here a wire of a very small radius (40 a.u.) has been deliberately chosen to better evidence the effect of the nonlocality of the response on the vdW interaction. Obviously, an experiment with a wire of such a small size is quite utopian. One may notice, however, that monolayer carbon nanotubes are not so far from such sizes. Since the anisotropy of the potential surface persists even for wires of a much larger radius (e.g., a few hundreds of a.u.), similar collisional effects should be seen, with larger cross sections, but within a smaller angular range (e.g., 10 times smaller, which keeps feasible an angular analysis). In order to enhance the scattering signal, a realistic experiment should be carried out with a beam of molecules traversing a transmission grating consisting of many parallel identical wires. Under such conditions, provided that the transverse coherence length is larger than the grating period, the *inelastic diffraction* of molecules could be observed, which would provide a higher sensitivity to inelastic processes and alignment effects. Owing to the rather small deflection angles involved here, a reflection grating consisting of parallel wires on a dielectric substrate should be used as well. This configuration would need however a new calculation of the interaction potential.

IV. CONCLUSION AND PERSPECTIVES

We have calculated anisotropic inductive and dispersive contributions to the vdW interaction between a molecule and a metallic nanowire in the mean distance range (12 a.u. up to a few hundreds of a.u.). For the sake of clarity the present calculation has been limited to the (dominant) dipole-dipole terms, but higher-order multipole contributions could be calculated as well along the same principles. It should be emphasized that owing to the ''eigenmode'' method used here, exact and analytical expressions of the reflection factors are derived. In other words, the uncertainties remaining in our vdW potential energy surface could only come from (i) the validity of the hydrodynamic nonlocal dielectric function of the metal and the parameters in it and (ii) the molecule permanent dipole, if any, and polarizabilities.

The anisotropy of the potential surface is responsible for rotational transitions. This has been shown for nitrogen molecules (assimilated to rigid rotators) colliding with an aluminum nanowire in the thermal energy range. In these transitions, selection rules $\Delta J=0,2$, $\Delta M=0,\pm2$ hold. Starting from the lowest rotational state ($J=0$) we show that, because of the specific angular dependence of the potential (i.e., the symmetry breaking of the molecular states induced by the surface), states $|2, 0\rangle$ and $|2, \pm2\rangle$ are unequally populated, i.e., that molecules in states $J=2$ are aligned. The degree of alignment gently oscillates, with a period of about 5°, as a function of the deflection angle, an effect that should be easily observed in an experiment.

As it can be seen in the above example [Figs. 4(b) and 5(a)], the transition probabilities from $J=0$ to $J=2$ are rather important (a few 10%). This means that the nanowire plays the role of an efficient beam splitter, a role that can be exploited in a molecular interferometric device similar to the so-called Stern-Gerlach atomic interferometers.[21] In our calculation it has been assumed that all molecules in an incident monokinetic and parallel beam are in state $|0, 0\rangle$. This selection (in internal state and velocity) is equivalent to the *polarization* stage of a Stern-Gerlach interferometer. It can be realized, for instance, by using a supersonic nozzle expansion. Similarly, one final rotational state needs to be selected (the *analyzer* in a Stern-Gerlach interferometer). This can be achieved, for instance, with the use of an inhomogeneous electric field[22] or with a laser-induced transition.[23]

ACKNOWLEDGMENT

One of us (M.B.) thanks the Foundation Louis de Broglie for providing him with a financial support.

*Author to whom all correspondence should be addressed. Email address: baudon@lpl.univparis13.fr

[1] O. Keller, Phys. Rep. **268**, 85 (1996).
[2] E. M. Lifshitz, Zh. Eksp. Teor. Fiz. **29**, 94 (1955) [Sov. Phys. JETP **2**, 72 (1956)]; D. Meschede, W. Jhe, and E. A. Hinds, Phys. Rev. A **41**, 1587 (1990).
[3] M. Boustimi, J. Baudon, J. Robert, A. Semlali, and B. Labani, Phys. Rev. B **62**, 7593 (2000).
[4] P. Fouquet *et al.* (unpublished).
[5] H. Failache *et al.*, Phys. Rev. Lett. **83**, 5467 (1999).
[6] M. Boustimi, B. Viaris de Lesegno, J. Baudon, J. Robert, and M. Ducloy, Phys. Rev. Lett. **86**, 2766 (2001).
[7] M. Boustimi, J. Baudon, F. Pirani, M. Ducloy, J. Reinhardt, F. Perales, C. Mainos, V. Bocvarski, and J. Robert, Europhys. Lett. **56**, 644 (2001).
[8] K. A. Williams, B. K. Pradhan, P. C. Eklund, M. K. Kostov, and M. W. Cole, Phys. Rev. Lett. **88**, 165502 (2002).
[9] V. S. Letokhov, in *Quantum Optics of Confined Systems*, Vol. 314

of *NATO Advanced Study Institute, Series E*, edited by M. Ducloy and D. Bloch (Kluwer Academic, Dordrecht, 1996), p. 327.

[10] J. Denschlag, D. Cassettari, and J. Schmiedmayer, Phys. Rev. Lett. **82**, 2014 (1999).

[11] H. J. Loesch, Chem. Phys. **207**, 427 (1996); H. J. Loesch and B. Scheel, Phys. Rev. Lett. **85**, 2709 (2000).

[12] R. Kubo, J. Phys. Soc. Jpn. **12**, 570 (1957); D. M. Newns, Phys. Rev. B **1**, 3304 (1970).

[13] M. Boustimi, J. Baudon, P. Candori, and J. Robert, Phys. Rev. B **65**, 155402 (2002).

[14] M. Boustimi, J. Baudon, and J. Robert, Opt. Commun. **198**, 389 (2001).

[15] A. D. McLachlan, Proc. R. Soc. London, Ser. A **271**, 387 (1963); Mol. Phys. **7**, 381 (1964); C. Girard, S. Maghezzi, and F. Hache, J. Chem. Phys. **91**, 5509 (1989).

[16] B. Labani, M. Boustimi, and J. Baudon, Phys. Rev. B **55**, 4745 (1997).

[17] M. Boustimi, Ph.D. thesis, University Chouaib Doukkali, El Jadida, Morocco, 1999.

[18] See, for instance, L. Landau and E. Lifchitz, *Mécanique Quantique*, 3rd ed. (Editions MIR, Moscow, 1974), Sec. 131.

[19] R. Campi, D. Cappelletti, G. Liuti, and F. Pirani, J. Chem. Phys. **95**, 1852 (1991).

[20] U. Buck, in *Atomic and Molecular Beam Methods*, edited by G. Scoles (Oxford University Press, New York, 1988), Vol. 1, p. 499.

[21] For a review, see J. Baudon, R. Mathevet, and J. Robert, J. Phys. B **32**, R173 (1999).

[22] J. Reuss, in *Atomic and Molecular Beam Methods* (Ref. 20), Vol. 1, p. 276.

[23] U. Hefter and K. Bergmann, in *Atomic and Molecular Beam Methods* (Ref. 20), p. 193 and references therein.